

# Revisiting Classifier: Transferring Vision-Language Models for Video Recognition

Wenhao Wu<sup>1,2</sup>Zhun Sun<sup>1</sup>Wanli Ouyang<sup>2,3\*</sup><sup>1</sup>Baidu Inc.<sup>2</sup>The University of Sydney<sup>3</sup>Shanghai AI Laboratory

whwu.ucas@gmail.com

## Abstract

Transferring knowledge from task-agnostic pre-trained deep models for downstream tasks is an important topic in computer vision research. Along with the growth of computational capacity, we now have open-source vision-language pre-trained models in large scales of the model architecture and amount of data. In this study, we focus on transferring knowledge for video classification tasks. Conventional methods randomly initialize the linear classifier head for vision classification, but they leave the usage of the text encoder for downstream visual recognition tasks undiscovered. In this paper, we revise the role of the linear classifier and replace the classifier with different knowledge from the pre-trained model. We utilize the well-pre-trained language model to generate a good semantic target for efficient transferring learning. The empirical study shows that our method improves both the performance and the training speed of video classification, with a negligible change in the model. Our simple yet effective tuning paradigm achieves state-of-the-art performance and efficient training on various video recognition scenarios, i.e., zero-shot, few-shot, and general recognition. In particular, our paradigm achieves the state-of-the-art accuracy of 87.8% on Kinetics-400, and also surpasses previous methods by 20~50% absolute top-1 accuracy under zero-shot, few-shot settings on five popular video datasets. Code and models can be found at <https://github.com/whwu95/Text4Vis>.

## 1. Introduction

Pre-training a task-agnostic model using large-scale general datasets and then transferring its learning feature representations to downstream tasks is a paradigm in many computer vision applications. While in the last decade, the convolutional-based models that are optimized on the ImageNet [9] dataset with a supervised style dominated this field. Owing to the dramatically increasing computational

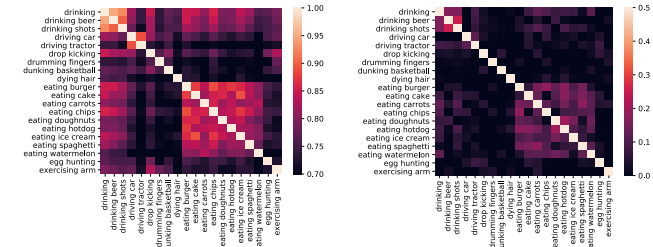


Figure 1. Inter-class correlation maps of “embeddings of class labels” for 20 categories on Kinetics-400. **Left:** The extracted textual vectors of class labels, **Right:** The “embeddings” from learned classifier. The color thresholds are adjusted for a better view. Please zoom in for the best view.

capacity, now we can train models that have several magnitude more model parameters and FLOPs on various image and even video datasets in either supervised [49] or self-supervised [12, 19, 21, 47] style. Recently, contrastive-based vision-language pre-training [42] manifest their superior capabilities in improving downstream tasks performance such as classification [42], captioning [39], image generation [43], to name a few. These models are powerful for two reasons: i) the employed large-scale weakly-related datasets provide rich semantics and diverse representations of concepts; ii) the representation vectors of images and texts are roughly aligned in the semantic embedding space. However, the most common approach to using these models is fine-tuning the visual encoder on specific tasks. Although the rich semantics and diverse representations of concepts benefit the downstream tasks, the usage of the textual encoder is still left overlooked.

In this study, we aim to improve the transferability of such vision-language pre-training models for downstream classification tasks, with the help of their textual encoders. Our motivation comes from the semantic similarity among the ground-truth labels. To demonstrate this, we employ the Kinetics video recognition dataset [26] for the analysis. We extract the embedded textual vectors of class labels using

\*Corresponding author.

the textual encoder of CLIP. We then calculate the correlation between the embedded textual vectors. The plot is shown on the left of Figure 1. Not surprisingly, the extracted textual vectors of class labels exhibit certain inter-class correlations since part of them include the same verbs in their labels, *e.g.*, *playing <something>*. Meanwhile, the labels with different verbs show a negligible inter-class correlation, *e.g.*, *drinking* and *driving*.

Next, we examine the final projection head of a vanilla video recognition framework. We conduct the visual-only fine-tuning process with the visual encoder that is also released by CLIP [42]. The detailed configurations are provided in Section 4.3. The projection head is a matrix of  $d \times c$  to compute the pre-softmax values (or logits) from the  $d$ -dimensional feature vectors for the  $c$  classes. Non-rigorously, we can consider the  $d$ -dimensional row vectors as the embeddings of the class labels, allowing us to explore the inter-class correlation between these learned “embeddings”, as shown on the right side of Figure 1. Interestingly, these learned “embeddings” also reveal certain correlations after the training, despite being initialized randomly and optimized without knowing any textual information<sup>1</sup>.

Therefore, we suppose that the semantic information contained in the samples does correlate with inter-classes. Following this motivation, we replace the projection matrix with several variants: i) The projection matrix whose row vectors are randomly sampled (trivial correlation); ii) The projection matrix whose row vectors are orthogonal to each other (non-correlated); iii) The projection matrix that is initialized using the visual statistic knowledge to provide maximized the correlation between labels (see Section 2.2); iv) The projection matrix with fixed embedded textual vectors provides the “proper” correlation. In the empirical studies, we find that textual knowledge significantly improves the transferability of pre-trained models, regarding both the classification accuracy and the convergence speed. Our main contributions are summarized as follows:

- We build a new recognition paradigm to improve the transferability using visual knowledge and textual knowledge from the well-pre-trained vision-language model.
- We conduct extensive experiments on popular video datasets (*i.e.*, Kinetics-400 & 600, UCF-101, HMDB-51 and ActivityNet) to demonstrate the transferability of our solution in many types of transfer learning, *i.e.*, zero-shot / few-shot / general video recognition. Our approach democratizes the training on video datasets and achieves state-of-the-art performance on various video recognition settings, *e.g.*, 87.8% top-1 accuracy on Kinetics-400, and outperforms previous methods

<sup>1</sup>That is, optimized with cross-entropy loss with one-hot labels

by 20~50% absolute top-1 accuracy under zero-shot, few-shot settings.

## 2. Methodology

**Denotations.** In the paper, we use bold letters to denote Vector, and capital italic letters to denote Tensor or Matrix, *e.g.*, we employ  $\mathbf{z} \in \mathbb{R}^d$  to denote the feature vector extracted from a pre-trained model of dimension  $d$ , we employ  $W \in \mathbb{R}^{d \times c}$  to denote the projection matrix for the  $c$ -class linear classifier. Without ambiguity, we also use capital italic letters to denote the modality in subscripts, especially we employ  $V$  and  $T$  to denote the *Visual* modality and *Textual* modality, respectively. We further employ lowercase italic letters to denote functions or neural networks. For instance, we employ  $g_V(\cdot, \Theta_V)$  and  $g_T(\cdot, \Theta_T)$  to denote the visual and textual encoder, respectively. Besides, we employ calligraphic letters, *e.g.*,  $\mathcal{D}$ , to denote sets of elements.

### 2.1. Revisiting of Previous Tuning Paradigms

**Standard vision transferring paradigm.** As shown in Figure 2(a), we start with the most ordinary scenario, where a visual encoder model  $g_V$  is optimized using a large-scale dataset  $\mathcal{D}$  that contains visual samples with or without ground-truth labels. On our labeled downstream dataset  $\tilde{\mathcal{D}} = \{(\mathbf{x}_1, \mathbf{y}_1), (\mathbf{x}_2, \mathbf{y}_2), \dots\}$ , our empirical learning target can be written as

$$g_V^*, W^* = \underset{\Theta_V, W}{\operatorname{argmin}} \mathbb{E}_{\mathbf{x}, \mathbf{y} \sim \tilde{\mathcal{D}}} [H(\mathbf{y} | \sigma(W \cdot g_V(\mathbf{x})))], \quad (1)$$

where  $H(\hat{p}|p)$  stands for the CrossEntropy between the predicted distribution  $p$  and the ground-truth distribution  $\hat{p}$ ,  $\sigma$  denotes the softmax operation,  $W \in \mathbb{R}^{c \times d}$  denotes the linear projection matrix for classification. The formulation in Eq. 1 is a standard visual feature transferring paradigm, where the visual encoder  $g_V$  and the projection matrix (classifier)  $W$  are learned simultaneously.

**Vision-language learning paradigm.** As shown in Figure 2(b), we then review the contrastive learning paradigm of the vision-language models. This paradigm has been widely used for vision-language pre-training *i.e.*, CLIP [42], and also been extend to video-text fine-tuning, *i.e.*, ActionCLIP [57], CLIP4Clip [37]. Given a weakly related vision-language pair (*e.g.*, image-text, video-text) dataset  $\mathcal{D} = \{(\mathbf{x}_{V,1}, \mathbf{x}_{T,1}), (\mathbf{x}_{V,2}, \mathbf{x}_{T,2})\dots\}$ . With slight abuse of the notations, we employ the  $\mathbf{x}_V, \mathbf{x}_T$  to denote a mini-batch of size  $b$ , then we minimize the following target,

$$g_V^*, g_T^* = \underset{\Theta_V, \Theta_T}{\operatorname{argmin}} \mathbb{E}_{\mathbf{x}_V, \mathbf{x}_T \sim \tilde{\mathcal{D}}} [H(\mathcal{Q} | \sigma(g_V(\mathbf{x}_V)^T \cdot g_T(\mathbf{x}_T)))], \quad (2)$$

where  $\mathcal{Q}$  is the set that contains  $b$  one-hot labels of size  $c$ , with their  $1, 2, \dots, b$ -th element being 1 ( $b < c$ , denoting

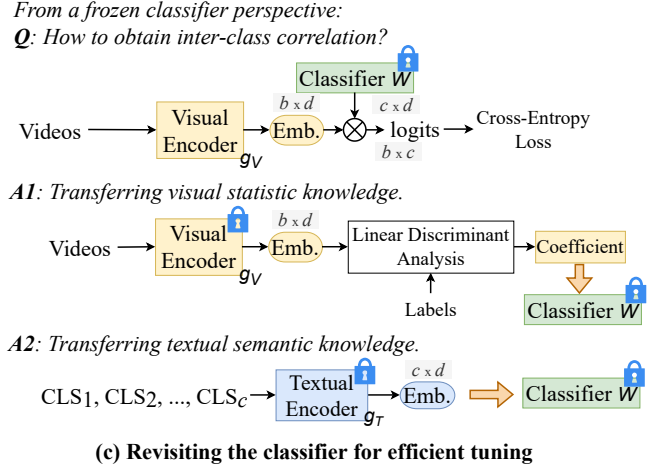
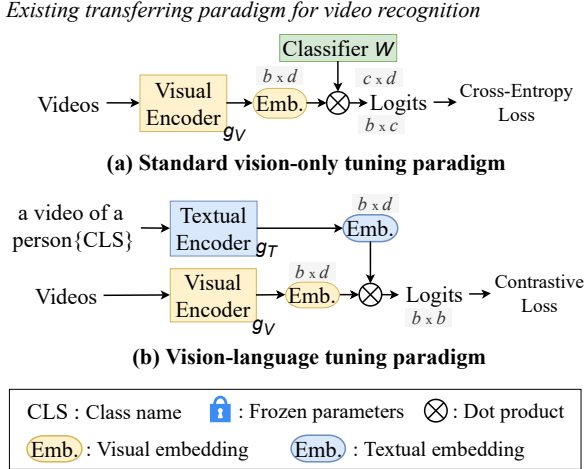


Figure 2. Illustration of transferring vision-language pre-trained models for video recognition. (a) The widely-used standard vision-only tuning paradigm with cross-entropy loss. (b) The vision-language tuning paradigm with contrastive loss. (c) Revisiting the role of the classifier to transfer knowledge from vision-language pre-trained models (e.g., CLIP).

the positive vision-language pairs. Here we clarify that, the definition in Eq. 2 is not the rigorous form of the Noise-Contrastive Estimation (NCE) loss proposed in [53]. Instead, we employ the cross entropy version implementation in [8, 42]. This implementation depicts a connection between the standard feature transferring paradigm and ours. In which the  $g_T(x_T)$  can be considered as the projection matrix that map the visual feature  $g_V(x_V)$  to the given label set  $\mathcal{Q}$ .

## 2.2. Our proposed paradigm

As discussed in Section 1, we replace the learnable randomly initialized linear projection matrix  $W$  with pre-defined matrix  $\tilde{W}$ . Similarly, the training target can be written as

$$g_V^* = \operatorname{argmin}_{\Theta_V} \mathbb{E}_{\mathbf{x}, \mathbf{y} \sim \tilde{\mathcal{D}}} [H(\mathbf{y} | \sigma(\tilde{W} \cdot g_V(\mathbf{x})))]. \quad (3)$$

Note that  $\tilde{W}$  is not in the optimization targets, since we freeze it from updating during the fine-tuning of the downstream tasks. We do this for two reasons: Firstly, it could preserve the textual knowledge from being disturbed by the randomness brought by the mini-batch. For instance, when some classes are missing, their embedded feature vector might be broken by the other classes; Secondly, we want to provide a fair comparison between different initialization of  $\tilde{W}$ . Now we consider how to initialize  $\tilde{W}$ . To examine how the correlation between the semantic information contained in the samples helps, we investigate the following four types of initialization, which represent different degrees of inter-class correlation.

**Randomized matrix** For the most simple randomized

matrix case, we set each row of the  $\tilde{W}$  with a random Gaussian vector of zero mean and standard deviation, that is

$$\tilde{W} \sim \mathcal{N}(\mathbf{0}, I_d), \quad (4)$$

where  $I_d$  denotes the identity matrix of dimension  $d \times d$ . Arithmetically, a trivial “correlation” would appear between the row of the  $\tilde{W}$ , since the sampling size is significantly small to be biased. Evidently, the trivial “correlation” cannot indicate the real correspondence between the classes due to its stochasticity. Therefore we expect the model to have inferior performance since it needs to avoid these incorrect correlations when learning the visual feature representation.

**Randomized Orthogonal matrix** We follow the approach of the randomized matrix. We then remove the correlation by ensuring the row vectors are orthogonal. This is achieved by QR decomposition. Concretely, since  $d > c$ , we first generate a random matrix of size  $d \times d$  and select the first  $c$  rows as our projection matrix. Formally, we have,

$$\begin{aligned} \tilde{W}_j &\sim \operatorname{QR}(U)_j, j = 1, 2, \dots, c, \\ U_i &\sim \mathcal{N}(\mathbf{0}, I_d), i = 1, 2, \dots, d, \end{aligned} \quad (5)$$

where  $U$  is the intermediate randomized matrix,  $\operatorname{QR}(U)$  is the row orthogonal matrix obtained through the QR decomposition. Similar to the randomized matrix, we also expect this initialization to have inferior performance. Given the fact that the one-hot label vectors are also orthogonal to each other, it will not be helpful to project the visual feature vectors with an orthogonal matrix, which increases the difficulty of learning meaningful visual features.

**Linear discriminant projection** We consider another way of initializing the projection matrix. We employ the

multi-class Fisher’s linear discriminant analysis (LDA) to learn a linear classifier, then employ the weight matrix of the classifier as our initialization of the projection matrix. Specifically, we use the pre-trained visual encoder to extract visual embeddings of samples in the train split, then perform LDA on the pre-extracted visual embeddings of the training set to generate the LDA coefficient. Finally, we use the LDA coefficient to initialize  $\tilde{W}$  and freeze it for fine-tuning the visual encoder on the dataset. We compute the LDA projection following previous work [31]. Intuitively, the LDA simultaneously maximizes the inter-class covariance and minimizes intra-class covariance. We, therefore, term this as the maximal correlation initialization using the visual statistic knowledge. As an essential classifier, this type of initialization delivers reasonable performance, but it is largely dependent on the data employed to compute the projection matrix. When the data is limited, the estimated correlation will be biased. On the other hand, in our proposed paradigm, the pre-trained textual encoder provides unbiased correlations for fine-tuning.

**Textual embedding vectors** We finally describe the paradigm to transfer textual semantic knowledge from a pre-trained textual encoder. Briefly, the projection weight  $\tilde{W}$  is composed of the embedded textual feature vectors of the labels. Given a set of tokenized class labels  $\mathcal{L} = \{\mathbf{l}_1, \mathbf{l}_2, \dots, \mathbf{l}_c\}$ , we have

$$\tilde{W}_i \sim g_T(\mathbf{l}_i), i = 1, 2, \dots, c, \quad (6)$$

where  $\tilde{W}_i$  the  $i$ -th row vector in matrix  $\tilde{W}$ . And  $\tilde{W}_i$  is initialized using the textual encoder output of the textual label of the  $i$ -th class. In the experimental analysis, we investigate two types of textual feature encoders: i) The encoder that is trained with a visual encoder in the contrastive style, *i.e.*, CLIP; ii) The encoder that is trained solely using only textual samples on tasks such as masked language modeling, *i.e.*, DistilBERT [45].

### 3. Related Works

**Visual Recognition.** Convolutional networks have long been the standard for backbone architectures in image recognition [20, 22, 28, 46] and video recognition [6, 41, 52, 65]. Inspired by the Transformer [54] scaling successes in Natural Language Processing, Vision Transformer (ViT) [10] applies a standard Transformer directly to images, which delivers impressive performance on image recognition. Since then, ViT [10] has led a new trend in image recognition backbone architectures, shifting from CNNs to Transformers. To improve performance, follow-up studies (*e.g.*, DeiT [18], Swin [34]) have been developed. Also, many works have begun to adopt transformers in video recognition, such as TimeSFormer [2], ViViT [1], VideoSwin [36], and MViT [11].

**Image-Language Pre-training.** Recently, CLIP [42] provides good practice in learning the coordinated vision-language pretraining models using the image-text InfoNCE contrastive loss [53]. Based on CLIP, several variants [23, 30, 68, 69] have been proposed by combining more types of learning tasks such as image-text matching and masked image/language modeling. These contrastively learned models have two deserved properties for downstream tasks: the abundant visual feature representations and the aligned textual feature representations. Yet another study [67] merged the downstream classification task into the pretraining progress, which demonstrates a decent improvement of accuracy over the standard cross-entropy loss.

**Transferring CLIP Models for Video-Text Learning.** Recently, many video-text retrieval methods [37, 59, 72] have benefited from vision-language pre-training as well. Moreover, ActionClip [57] and VideoPrompt [25] extend CLIP [42] to train a downstream video-text matching model with contrastive loss, then perform video recognition using the similarity between learned video and text embeddings during inference. Instead of these contrastive-based methods, we investigate the correlations of the linear classifier for efficient feature transferring in the standard visual recognition paradigm. Then we directly transfer visual and textual knowledge for video recognition. In comparison to contrastive-based methods, we demonstrate the superiority of our method in efficient training in Table 9. More recently, we notice a concurrent work X-CLIP [40], which was released a month later than our initial arXiv version<sup>2</sup>, and also transfers CLIP to video recognition with cross-entropy loss. We hope that this simple and effective paradigm can serve as a new baseline for future work.

## 4. Experiments: Video Recognition

### 4.1. Setups

To evaluate our method for video recognition, we conduct experiments on five popular datasets, *i.e.*, Kinetics-400 [26], Kinetics-600 [5], UCF-101 [48], HMDB-51 [29] and ActivityNet-v1.3 [4]. See Appendix §C.1 for statistics of these datasets.

**Training.** The video recognition task takes a video as input, and then feed it into a learned encoder to estimate the action category of the video. Given a video, we first uniformly sample  $T$  (*e.g.*, 8, 16, 32) frames over the entire video. Then we utilize ResNet [20] or ViT [10] as the video encoders. The classifier in our paradigm is initialized from the textual embedding of the class names and then frozen (fixed), leaving only the parameters in the video encoder to be learned. See Appendix B.1 for training hyperparameters.

**Inference.** To trade off accuracy and speed, we consider two inference strategies: (1) *Single View*: We use only 1 clip

<sup>2</sup><https://arxiv.org/abs/2207.01297v1>

Method	Input	Pre-train	Top-1	Top-5	FLOPs×Views	Param
NL I3D-101 [58]	128×224 <sup>2</sup>	IN-1K	77.7	93.3	359×10×3	61.8
MVFNet <sub>En</sub> [60]	24×224 <sup>2</sup>	IN-1K	79.1	93.8	188×10×3	-
SlowFast NL101 [14]	16×224 <sup>2</sup>	Scratch	79.8	93.9	234×10×3	59.9
X3D-XXL [13]	16×440 <sup>2</sup>	Scratch	80.4	94.6	144×10×3	20.3
MViT-B, 64×3 [11]	64×224 <sup>2</sup>	Scratch	81.2	95.1	455×3×3	36.6
<i>Methods with large-scale pre-training</i>						
TimeSformer-L [2]	96×224 <sup>2</sup>	IN-21K	80.7	94.7	2380×1×3	121.4
ViViT-L/16×2 [1]	32×320 <sup>2</sup>	IN-21K	81.3	94.7	3992×4×3	310.8
VideoSwin-L [36]	32×384 <sup>2</sup>	IN-21K	84.9	96.7	2107×10×5	200.0
ip-CSN-152 [51]	32×224 <sup>2</sup>	IG-65M	82.5	95.3	109×10×3	32.8
ViViT-L/16×2 [1]	32×320 <sup>2</sup>	JFT-300M	83.5	95.5	3992×4×3	310.8
ViViT-H/16×2 [1]	32×224 <sup>2</sup>	JFT-300M	84.8	95.8	8316×4×3	647.5
TokLearner-L/10 [44]	32×224 <sup>2</sup>	JFT-300M	85.4	96.3	4076×4×3	450
MTV-H [66]	32×224 <sup>2</sup>	JFT-300M	85.8	96.6	3706×4×3	-
CoVeR [71]	16×448 <sup>2</sup>	JFT-300M	86.3	-	-×1×3	-
Florence [69]	32×384 <sup>2</sup>	FLD-900M	86.5	97.3	-×4×3	647
CoVeR [71]	16×448 <sup>2</sup>	JFT-3B	87.2	-	-×1×3	-
VideoPrompt ViT-B/16 [25]	16×224 <sup>2</sup>	WIT-400M	76.9	93.5	-	-
ActionCLIP ViT-B/16 [57]	32×224 <sup>2</sup>	WIT-400M	83.8	96.2	563×10×3	141.7
Ours ViT-L/14	32×224 <sup>2</sup>	WIT-400M	87.1	97.4	1662×4×3	230.7
Ours ViT-L/14	32×336 <sup>2</sup>	WIT-400M	<b>87.8</b>	<b>97.6</b>	3829×1×3	230.7

Table 1. Comparisons with SOTAs on Kinetics-400. “Views” indicates # temporal clip × # spatial crop. The magnitudes are Giga ( $10^9$ ) and Mega ( $10^6$ ) for FLOPs and Param. “IN” denotes ImageNet.

Method	Top-1	mAP
ListenToLook [16]	-	89.9
MARL [61]	85.7	90.1
DSANet [62]	-	90.5
TSQNet [63]	88.7	93.7
NSNet [64]	90.2	94.3
Ours ViT-L	<b>92.9</b>	<b>96.5</b>
Ours ViT-L (336↑)	<b>93.3</b>	<b>96.9</b>

Table 2. Comparisons with SOTAs on ActivityNet.

per video and the center crop for efficient evaluation, (*e.g.*, as in Sec. 4.3). (2) *Multiple Views*: This is a widely used setting in previous works [6, 14] to sample multiple clips per video with several spatial crops in order to get higher accuracy. For comparison with SOTAs, we use four clips with three crops (“4×3 Views”) in Table 1.

## 4.2. Main Results.

**Comparison to state-of-the-arts.** In Table 1, on the challenging **Kinetics-400** dataset, we compare to state-of-the-arts that are pre-trained on large-scale datasets such as ImageNet-21K [9], IG-65M [17], JFT-300M [49], FLD-900M [69] and JFT-3B [70]. Up to now, none of the three largest datasets (*i.e.*, JFT-300M, FLD-900M, JFT-3B) is open-sourced and also does not provide pre-trained mod-

Method	shot	HMDB	UCF	ANet	K400
VideoSwin [36]	2	20.9	53.3	-	-
VideoPrompt [25]	5	56.6	79.5	-	58.5
X-Florence [40]	2	51.6	84.0	-	-
Ours ViT-L	0	53.8	71.9	75.6	61.0
	1	<b>72.7</b>	<b>96.4</b>	<b>89.0</b>	<b>75.8</b>
	2	<b>73.5</b>	<b>96.6</b>	<b>90.3</b>	<b>78.2</b>
All	80.1	96.9	91.1	84.7	

Table 3. Comparisons with SOTAs on few-shot action recognition.

els. Thus, we use the CLIP [42] checkpoints, which are publicly available<sup>3</sup> and have been trained on 400 million web image-text pairs (namely WIT-400M). We can observe that our model outperforms all JFT-pretrained methods in terms of Top-1 and Top-5 accuracy. We achieve an accuracy of 87.8%, which improves even further by 1.3% over Florence [69], although their model and data scale are both 2× larger than ours. Besides, our model is even better than CoVeR [71], and its data scale is 7.5× larger.

To verify the generalization ability of our method, we further evaluate the performance of our method on the well-known untrimmed video benchmark, **ActivityNet-v1.3**. We finetuned the Kinetics-400 pre-trained models

<sup>3</sup><https://github.com/openai/CLIP/blob/main/clip/clip.py>

Method	UCF* / UCF	HMDB* / HMDB	ANet* / ANet	Kinetics-600
GA [38]	17.3±1.1 / -	19.3±2.1 / -	-	-
TS-GCN [15]	34.2±3.1 / -	23.2±3.0 / -	-	-
E2E [3]	44.1 / 35.3	29.8 / 24.8	26.6 / 20.0	-
DASZL [27]	48.9±5.8 / -	- / -	-	-
ER [7]	51.8±2.9 / -	35.3±4.6 / -	-	42.1±1.4
ResT [32]	58.7±3.3 / 46.7	41.1±3.7 / 34.4	32.5 / 26.3	-
Ours	<b>85.8±3.3 / 79.6</b>	<b>58.1±5.7 / 49.8</b>	<b>84.6±1.4 / 77.4</b>	<b>68.9±1.0</b>

Table 4. Comparisons with SOTAs on zero-shot video recognition. We directly evaluate our method without any additional training on cross-dataset video recognition. ANet is in short for ActivityNet. \* means half classes evaluation.

Method	UCF-101	HMDB-51
ARTNet [55]	94.3%	70.9%
I3D [6]	95.6%	74.8%
R(2+1)D [52]	96.8%	74.5%
S3D-G [65]	96.8%	75.9%
TSM [33]	95.9%	73.5%
STM [24]	96.2%	72.2%
TEINet [35]	96.7%	72.1%
MVFNet [60]	96.6%	75.7%
TDN [56]	97.4%	76.4%
Ours ViT-L	<b>98.1%</b>	<b>81.3%</b>
Ours ViT-L (336↑)	<b>98.2%</b>	<b>81.3%</b>

Table 5. **Mean class accuracy** on UCF-101 and HMDB-51 achieved by different methods which are transferred from their **Kinetics** models with RGB modality.

with 8 frames on the Activitynet-v1.3 dataset and report the top-1 accuracy and mean average precision (mAP) following the official evaluation metrics. As shown in Table 2, our method outperforms recent SOTAs with a clear margin. To the best of our knowledge, our method achieves the best performance (96.9%) on ActivityNet.

We also evaluate our method on the **UCF-101** and **HMDB-51** datasets to demonstrate its capacity to generalize to smaller data. We finetune our models on these two datasets using the pre-trained ViT-L model on Kinetics-400 and present the mean class accuracy on split one. We utilize 16 frames as inputs and 30 epochs for training. Table 5 reveals that our model has a pretty transfer capability, with mean class accuracy of 98.2% on UCF-101 and 81.3% on HMDB-51, respectively.

**Few-shot video recognition.** Video recognition using only a few samples is known as few-shot video recognition. We study a more challenging  $K$ -shot  $C$ -way situation instead of the conventional 5-shot 5-way configuration. We scale the task up to categorize **all** categories in the dataset with just  $K$  samples per category for training. The lower and upper bound of this situation are denoted by the term “Zero-

shot” and “All-shot” respectively. Table 3 reports the Top-1 accuracy for the four datasets. In this extreme scenario of few data, we use CLIP-pretrained ViT-L/14 with 8 frames and TAP for few-shot video recognition. In these extremely data-poor situations (*e.g.*, even with just one shot), we can see that our method offers amazing transferability to diverse domain data. Our approach, in contrast, demonstrates robustness by outperforming SOTAs by a large margin. For instance, when comparing accuracy on HMDB-51 with 2-shot, our method outperforms Swin, X-Florence by **+56.9%** and **+26.2%** respectively. *See Appendix B.1 for training details.*

**Zero-shot video recognition.** Furthermore, we conduct experiments in the open-set setting. We use our Kinetics-400 pre-trained models to perform the zero-shot evaluation on four other video datasets. On UCF-101, HMDB-51 and ActivityNet, there are two evaluation protocols following [3]:

1. In order to make our results comparable with previous works, we randomly choose half of the test dataset’s classes, 50 for UCF, 25 for HMDB, and 100 for ActivityNet. Evaluate on the selected subset. Repeat ten times and average the results for each test dataset. We denote this setting as UCF\*, HMDB\* and ANet\*.
2. The second evaluation setting is directly evaluating on the full dataset. This allows us to return more realistic accuracy scores.

On Kinetics-600, we follows [7] to choose the 220 new categories outside Kinetics-400 in Kinetics-600 for evaluation. We use the three splits provided by [7]. For each split, we sample 160 categories for evaluation from the 220 categories in Kinetics-600. We report the mean accuracy for three splits. We present comprehensive comparisons on four datasets in Table 4, our method demonstrates a strong cross-dataset generalization ability. Our method shows a large improvement upon previous zero-shot video recognition methods (**+27.1%** on UCF-101, **+17.0%** on HMDB-51, **+52.1%** on ActivityNet, **+26.8%** on Kinetics-600).

### 4.3. Ablations on Kinetics.

In this section, we conduct extensive ablation experiments on the Kinetics-400 dataset. Unless specified otherwise, we use ViT-B/16 with 8 frames as the video backbone and a single view for testing. The default settings are marked in gray. *See Appendix B.2 for more ablations.*

**Different initializations to the offline classifier.** We set different initializations described in Section 2.2 to the offline classifier  $W \in \mathbb{R}^{d \times c}$  and then train our visual encoder on Kinetics-400. Table 6 lists their comparisons. We show that feeding the offline classifier a random  $d$ -by- $c$  matrix with a normal distribution reduces performance significantly. Then we assign the orthogonal matrix to the classifier, and see that removing the inter-class correlation of the classifier will result in inferior performance. Furthermore, we term the linear discriminate projection as the maximal correlation initialization. To do so, we first sample 60 videos from each class in the training set and utilize the pre-trained visual encoder to extract visual embeddings from these 24,000 videos. Finally, we learn the linear classifier by performing linear discriminant analysis on these visual embeddings and their labels. We can see the LDA projection achieves a strong baseline.

Finally, we study the textual embeddings from different textual encoders. We choose DistilBERT [45] and CLIP [42] as the textual encoder to pre-extract the text embeddings of  $c$  categories. We observe that DistilBERT performs the same performance as CLIP’s textual encoder. This may be because both DistillBERT and CLIP are pre-trained with large-scale data, so they both have strong language modeling capabilities and can generate good semantic targets. Although the good semantic targets generated by DistillBERT are not aligned with the visual features of CLIP, it is easy to fit them with trainable visual encoders. We also observe that the loss of DistillBERT will be higher than CLIP in the early stage, but it will quickly decrease to the same level. *More visualizations of these classifiers are in Appendix B.3.*

Offline classifier from	Top 1
Random normal matrix	59.3
Random orthogonal matrix	59.4
Linear discriminant projection	80.8
DistilBERT	81.4
Textual encoder of CLIP	<b>81.5</b>

Table 6. Exploration of different frozen classifiers.

**Comparison with vision-only tuning paradigm.** As a comparison with our method, we train the unimodality video model, which consists of the same visual encoder and a learnable classifier with random initialization. To produce

video embedding, we just apply temporal average pooling (TAP) to frame embeddings. As shown in Table 7, our *Vision-Text* method leads to obvious improvement with the same training recipe, especially in the data-poor situation. *See Appendix B.2 for more comparison figures.*

	Zero-shot	2-shot	Full-shot
<i>Vision-Only</i>	0.2	43.6	75.27
<i>Vision-Text</i>	<b>54.2</b>	<b>66.4</b>	<b>80.13</b>

Table 7. Comparisons with vision-only framework.

**Temporal modeling.** Here we explore more temporal modelings for ViT and ResNet: (1) **TAP**: Temporal average pooling is the most straightforward temporal modeling. (2) **T1D**: The channel-wise temporal 1D convolutions, is a common strategy [35, 56, 60], to perform efficient temporal interaction in the latter stages (*i.e.*,  $\text{res}_{4-5}$ ) of ResNet. (3) **T-Trans**: The embeddings of frames are fed to a multi-layer (*e.g.*, 6-layer) temporal transformer encoder. (4) **TokenT1D**: We use T1D to model temporal relations for [class] token features that are aggregated from local features via attention in the vision transformer. We perform the TokenT1D in multiple positions of a vision transformer. Results are shown in Table 8. On both backbones, TAP provides simple baselines and T-Trans exhibits the best top-1 accuracy. Both of them maintain the original frame-level representations and then perform temporal modeling. An interesting thing we observed is that T1D does not seem to work in this scenario. The reason lies in that T1D may have the potential to break the learned strong representations provided by CLIP. TokenT1D is another internal-backbone temporal modeling, and it does not yield a performance drop, and even slightly improves the TAP baseline. We believe this is because TokenT1D is only imposed on the global [class] token features instead of patch features, resulting in minimal modifications on pre-trained features.

Backbone	Modeling	Top-1	Top-5
ResNet-50	TAP	71.2	90.4
	T1D	67.2	88.5
	T-Trans	<b>74.3</b>	<b>91.7</b>
ViT-B/16	TAP	80.1	95.0
	TokenT1D	80.4	95.0
	T-Trans	<b>81.5</b>	<b>95.5</b>

Table 8. Temporal modeling for video encoders.

**Ours v.s. Contrastive-based paradigm.** We make a comparison with the Contrastive-based tuning method *i.e.*, ActionClip [57] mentioned in Section 3. This paradigm treats

the recognition task as a video-text matching problem with contrastive loss, thus requiring a batch gathering to collect embeddings of all batches across all GPUs and calculate cosine similarity for a given batch across all other batches. To be fair, we follow the public official code and configurations of ActionCLIP [57] for the experiments. And our recognition paradigm of course uses the Cross-Entropy loss to train the model. In Table 9, we compare it with the Contrastive-based paradigm and observe that it does not work well without batch gathering. This is due to contrastive learning favors a large batch size. (e.g., CLIP [42] used 256 GPUs with a batch size of 128 per GPU to maintain a large  $32768 \times 32768$  similarity matrix). Besides, involving batch gather will multiply the training time. Also, in this case, the pre-trained textual encoder still needs to be updated, which requires larger GPU memory. However, our paradigm employs pre-extracted text embeddings as our classifier, so the only learned part is the visual encoder. Results show that our method achieves the best accuracy-cost trade-off. Specifically, our method achieves the performance of 81.5% with ViT-B/16, which takes only 10 hours to run the training using 8 GPUs (**2× faster** than the matching counterpart). See Appendix §C.3 for details about the batch gathering.

Paradigm	Batch Gather	Textual Encoder	Top-1	V100-days
Contrastive- Based	✓	online	81.2	6.7 (10*)
	✓	offline	80.7	6.6
	✗	online	77.8	3.5
	✗	offline	76.1	3.3
Ours	✗	offline	<b>81.5</b>	<b>3.3</b>

Table 9. Ours vs. Contrastive-based paradigm with ViT-B/16 on Kinetics-400. The number of V100 days is the number of V100 GPU used for training multiplied by the training time in days. \* indicates the official result [57] via “Data-parallel training” on 3090 GPUs. For efficient training and fair comparison, we implement all experiments with “Distributed Data-parallel training”.

**More instantiations.** We assess different instantiations of our method, in terms of different visual encoders and more input frames. In Table 11, we present the results of our method with different architectures. In general, more frames, larger spatial resolution, and deeper backbones lead to higher accuracy. In Table 10, we provide the results of two typical evaluation protocols mentioned in Sec. 4.1. See Appendix §C.2 for more details on architectures.

**Analysis on efficiency.** In Table 12, we present the computational cost and efficiency of our models. We follow the common inference settings by using a single NVIDIA A100 GPU to measure the throughput. We use a batch size of 16 to measure the throughput. Our models achieve the **29×**

Views	Top-1	GFLOPs
Single→Multiple	81.5→ <b>82.9</b>	<b>90.3</b> →90.3×12

Table 10. Two classic evaluation protocols.

Frames	ResNet50	ViT-B/32	ViT-B/16	ViT-L/14
8	75.5%	80.0%	82.9%	<b>86.4%</b>
16	76.6%	80.5%	83.6%	<b>86.7%</b>

Table 11. Instantiations with multiple views inference.

Method	Top-1	FLOPs	Params	Throughput
ViViT-L/16-320 [1]	81.3	3992G	310.8M	4.2 vid/s*
Ours ViT-B/32	78.5	23.7G	71.6M	322.5 vid/s
Ours ViT-B/16	81.5	90.3G	69.9M	126.5 vid/s
Ours ViT-L/14	85.4	415.4G	230.4M	35.5 vid/s

Table 12. Analysis on throughput. “vid/s” represents the average number of videos per second. The larger “vid/s” represents higher efficiency. \* is the official result with TPU-v3.

**faster** throughput and **44× fewer** FLOPs compared with the previous transformer-based method ViViT [1] under the same accuracy.

## 5. Limitation

The study still has some limitations which are worth diving into in future research. The performance of the proposed paradigm is restricted to how the category labels are represented. For instance, in tasks such as human re-identification, the labels are often set as numerical values such as 0, 1, 2, etc. In this case, we cannot transfer any semantic information from the textual encoders, while transferring visual statistic knowledge (*i.e.*, LDA classifier) could be helpful.

## 6. Conclusion

We present a new paradigm for improving the transferability of visual recognition that is based on the knowledge from the textual encoder of the well-trained vision-language model. The empirical study shows that our method improves both the performance and the convergence speed of visual classification. The proposed approach has superior performance on both general and zero-shot/few-shot recognition and achieves state-of-the-art performance on video recognition tasks, and democratizes transferring on challenging video datasets.

## Acknowledgments

Wanli Ouyang was supported by the Australian Research Council Grant DP200103223, Australian Medical Research Future Fund MRAFI000085, CRC-P Smart Material Recovery Facility (SMRF) – Curby Soft Plastics, and CRC-P ARIA - Bionic Visual-Spatial Prostheses for the Blind.

## References

- [1] Anurag Arnab, Mostafa Dehghani, Georg Heigold, Chen Sun, Mario Lučić, and Cordelia Schmid. Vivit: A video vision transformer. In *ICCV*, pages 6836–6846, 2021. [4](#), [5](#), [8](#)
- [2] Gedas Bertasius, Heng Wang, and Lorenzo Torresani. Is space-time attention all you need for video understanding? In *ICML*, pages 813–824. PMLR, 2021. [4](#), [5](#)
- [3] Biagio Brattoli, Joseph Tighe, Fedor Zhdanov, Pietro Perona, and Krzysztof Chalupka. Rethinking zero-shot video classification: End-to-end training for realistic applications. In *CVPR*, pages 4613–4623, 2020. [6](#)
- [4] Fabian Caba Heilbron, Victor Escorcia, Bernard Ghanem, and Juan Carlos Niebles. Activitynet: A large-scale video benchmark for human activity understanding. In *CVPR*, pages 961–970, 2015. [4](#), [13](#)
- [5] Joao Carreira, Eric Noland, Andras Banki-Horvath, Chloe Hillier, and Andrew Zisserman. A short note about kinetics-600. *arXiv preprint arXiv:1808.01340*, 2018. [4](#), [13](#)
- [6] Joao Carreira and Andrew Zisserman. Quo vadis, action recognition? a new model and the kinetics dataset. In *CVPR*, pages 6299–6308, 2017. [4](#), [5](#), [6](#)
- [7] Shizhe Chen and Dong Huang. Elaborative rehearsal for zero-shot action recognition. In *ICCV*, pages 13638–13647, 2021. [6](#)
- [8] Xinlei Chen, Saining Xie, and Kaiming He. An empirical study of training self-supervised vision transformers. In *ICCV*, pages 9640–9649, 2021. [3](#)
- [9] Jia Deng, Wei Dong, Richard Socher, Li-Jia Li, Kai Li, and Li Fei-Fei. Imagenet: A large-scale hierarchical image database. In *CVPR*, pages 248–255, 2009. [1](#), [5](#), [12](#)
- [10] Alexey Dosovitskiy, Lucas Beyer, Alexander Kolesnikov, Dirk Weissenborn, Xiaohua Zhai, Thomas Unterthiner, Mostafa Dehghani, Matthias Minderer, Georg Heigold, Sylvain Gelly, et al. An image is worth 16x16 words: Transformers for image recognition at scale. *arXiv preprint arXiv:2010.11929*, 2020. [4](#)
- [11] Haoqi Fan, Bo Xiong, Karttikeya Mangalam, Yanghao Li, Zhicheng Yan, Jitendra Malik, and Christoph Feichtenhofer. Multiscale vision transformers. In *ICCV*, pages 6824–6835, 2021. [4](#), [5](#)
- [12] Bo Fang, Wenhao Wu, Chang Liu, Yu Zhou, Dongliang He, and Weiping Wang. Mamico: Macro-to-micro semantic correspondence for self-supervised video representation learning. In *ACM MM*, pages 1348–1357, 2022. [1](#)
- [13] Christoph Feichtenhofer. X3d: Expanding architectures for efficient video recognition. In *CVPR*, pages 203–213, 2020. [5](#)
- [14] Christoph Feichtenhofer, Haoqi Fan, Jitendra Malik, and Kaiming He. Slowfast networks for video recognition. In *ICCV*, pages 6202–6211, 2019. [5](#)
- [15] Junyu Gao, Tianzhu Zhang, and Changsheng Xu. I know the relationships: Zero-shot action recognition via two-stream graph convolutional networks and knowledge graphs. In *AAAI*, volume 33, pages 8303–8311, 2019. [6](#)
- [16] Ruohan Gao, Tae-Hyun Oh, Kristen Grauman, and Lorenzo Torresani. Listen to look: Action recognition by previewing audio. In *CVPR*, pages 10457–10467, 2020. [5](#)
- [17] Deepti Ghadiyaram, Du Tran, and Dhruv Mahajan. Large-scale weakly-supervised pre-training for video action recognition. In *CVPR*, pages 12046–12055, 2019. [5](#)
- [18] Kai Han, An Xiao, Enhua Wu, Jianyuan Guo, Chunjing Xu, and Yunhe Wang. Transformer in transformer. *NeurIPS*, pages 15908–15919, 2021. [4](#), [12](#)
- [19] Kaiming He, Haoqi Fan, Yuxin Wu, Saining Xie, and Ross Girshick. Momentum contrast for unsupervised visual representation learning. In *CVPR*, pages 9729–9738, 2020. [1](#)
- [20] Kaiming He, Xiangyu Zhang, Shaoqing Ren, and Jian Sun. Deep residual learning for image recognition. In *CVPR*, pages 770–778, 2016. [4](#)
- [21] Deng Huang, Wenhao Wu, Weiwen Hu, Xu Liu, Dongliang He, Zhihua Wu, Xiangmiao Wu, Mingkui Tan, and Errui Ding. Ascnet: Self-supervised video representation learning with appearance-speed consistency. In *ICCV*, pages 8096–8105, 2021. [1](#)
- [22] Sergey Ioffe and Christian Szegedy. Batch normalization: Accelerating deep network training by reducing internal covariate shift. In *ICML*, pages 448–456. PMLR, 2015. [4](#)
- [23] Chao Jia, Yinfen Yang, Ye Xia, Yi-Ting Chen, Zarana Parekh, Hieu Pham, Quoc Le, Yun-Hsuan Sung, Zhen Li, and Tom Duerig. Scaling up visual and vision-language representation learning with noisy text supervision. In *ICML*, pages 4904–4916. PMLR, 2021. [4](#)
- [24] Boyuan Jiang, MengMeng Wang, Weihao Gan, Wei Wu, and Junjie Yan. Stm: Spatiotemporal and motion encoding for action recognition. In *ICCV*, pages 2000–2009, 2019. [6](#)
- [25] Chen Ju, Tengda Han, Kunhao Zheng, Ya Zhang, and Weidi Xie. Prompting visual-language models for efficient video understanding. In *ECCV*, pages 105–124. Springer, 2022. [4](#), [5](#)
- [26] Will Kay, Joao Carreira, Karen Simonyan, Brian Zhang, Chloe Hillier, Sudheendra Vijayanarasimhan, Fabio Viola, Tim Green, Trevor Back, Paul Natsev, et al. The kinetics human action video dataset. *arXiv preprint arXiv:1705.06950*, 2017. [1](#), [4](#), [13](#)
- [27] Tae Soo Kim, Jonathan Jones, Michael Peven, Zihao Xiao, Jin Bai, Yi Zhang, Weichao Qiu, Alan Yuille, and Gregory D Hager. Daszl: Dynamic action signatures for zero-shot learning. In *AAAI*, volume 35, pages 1817–1826, 2021. [6](#)
- [28] Alex Krizhevsky, Ilya Sutskever, and Geoffrey E Hinton. Imagenet classification with deep convolutional neural networks. *NeurIPS*, 25, 2012. [4](#)
- [29] Hildegarde Kuehne, Hueihan Jhuang, Estibaliz Garrote, Tomaso Poggio, and Thomas Serre. Hmdb: a large video database for human motion recognition. In *ICCV*, pages 2556–2563, 2011. [4](#), [13](#)

[30] Junnan Li, Dongxu Li, Caiming Xiong, and Steven Hoi. Blip: Bootstrapping language-image pre-training for unified vision-language understanding and generation. *arXiv preprint arXiv:2201.12086*, 2022. 4

[31] Tao Li, Shenghuo Zhu, and Mitsunori Ogihara. Using discriminant analysis for multi-class classification: an experimental investigation. *Knowledge and information systems*, 10(4):453–472, 2006. 4

[32] Chung-Ching Lin, Kevin Lin, Lijuan Wang, Zicheng Liu, and Linjie Li. Cross-modal representation learning for zero-shot action recognition. In *CVPR*, pages 19978–19988, 2022. 6

[33] Ji Lin, Chuang Gan, and Song Han. Tsm: Temporal shift module for efficient video understanding. In *ICCV*, 2019. 6

[34] Ze Liu, Yutong Lin, Yue Cao, Han Hu, Yixuan Wei, Zheng Zhang, Stephen Lin, and Baining Guo. Swin transformer: Hierarchical vision transformer using shifted windows. In *ICCV*, pages 10012–10022, 2021. 4

[35] Zhaoyang Liu, Donghao Luo, Yabiao Wang, Limin Wang, Ying Tai, Chengjie Wang, Jilin Li, Feiyue Huang, and Tong Lu. Teinet: Towards an efficient architecture for video recognition. In *AAAI*, pages 11669–11676, 2020. 6, 7

[36] Ze Liu, Jia Ning, Yue Cao, Yixuan Wei, Zheng Zhang, Stephen Lin, and Han Hu. Video swin transformer. In *CVPR*, pages 3202–3211, 2022. 4, 5

[37] Huaishao Luo, Lei Ji, Ming Zhong, Yang Chen, Wen Lei, Nan Duan, and Tianrui Li. Clip4clip: An empirical study of clip for end to end video clip retrieval. *arXiv preprint arXiv:2104.08860*, 2021. 2, 4

[38] Ashish Mishra, Vinay Kumar Verma, M Shiva Krishna Reddy, S Arulkumar, Piyush Rai, and Anurag Mittal. A generative approach to zero-shot and few-shot action recognition. In *WACV*, pages 372–380. IEEE, 2018. 6

[39] Ron Mokady, Amir Hertz, and Amit H Bermano. Clipcap: Clip prefix for image captioning. *arXiv preprint arXiv:2111.09734*, 2021. 1

[40] Bolin Ni, Houwen Peng, Minghao Chen, Songyang Zhang, Gaofeng Meng, Jianlong Fu, Shimeng Xiang, and Haibin Ling. Expanding language-image pretrained models for general video recognition. In *ECCV*, pages 1–18. Springer, 2022. 4, 5

[41] Zhaofan Qiu, Ting Yao, and Tao Mei. Learning spatio-temporal representation with pseudo-3d residual networks. In *ICCV*, pages 5533–5541, 2017. 4

[42] Alec Radford, Jong Wook Kim, Chris Hallacy, Aditya Ramesh, Gabriel Goh, Sandhini Agarwal, Girish Sastry, Amanda Askell, Pamela Mishkin, Jack Clark, et al. Learning transferable visual models from natural language supervision. In *ICML*, pages 8748–8763. PMLR, 2021. 1, 2, 3, 4, 5, 7, 8

[43] Aditya Ramesh, Mikhail Pavlov, Gabriel Goh, Scott Gray, Chelsea Voss, Alec Radford, Mark Chen, and Ilya Sutskever. Zero-shot text-to-image generation. In *ICML*, pages 8821–8831. PMLR, 2021. 1

[44] Michael S Ryoo, AJ Piergiovanni, Anurag Arnab, Mostafa Dehghani, and Anelia Angelova. Tokenlearner: What can 8 learned tokens do for images and videos? *arXiv preprint arXiv:2106.11297*, 2021. 5

[45] Victor Sanh, Lysandre Debut, Julien Chaumond, and Thomas Wolf. Distilbert, a distilled version of bert: smaller, faster, cheaper and lighter. *arXiv preprint arXiv:1910.01108*, 2019. 4, 7

[46] Karen Simonyan and Andrew Zisserman. Very deep convolutional networks for large-scale image recognition. *arXiv preprint arXiv:1409.1556*, 2014. 4

[47] Yuxin Song, Min Yang, Wenhao Wu, Dongliang He, Fu Li, and Jingdong Wang. It takes two: Masked appearance-motion modeling for self-supervised video transformer pre-training. *arXiv preprint arXiv:2210.05234*, 2022. 1

[48] Khurram Soomro, Amir Roshan Zamir, and Mubarak Shah. Ucf101: A dataset of 101 human actions classes from videos in the wild. *arXiv preprint arXiv:1212.0402*, 2012. 4, 13

[49] Chen Sun, Abhinav Shrivastava, Saurabh Singh, and Abhinav Gupta. Revisiting unreasonable effectiveness of data in deep learning era. In *ICCV*, pages 843–852, 2017. 1, 5

[50] Ilya O Tolstikhin, Neil Houlsby, Alexander Kolesnikov, Lucas Beyer, Xiaohua Zhai, Thomas Unterthiner, Jessica Yung, Andreas Steiner, Daniel Keysers, Jakob Uszkoreit, et al. Mlp-mixer: An all-mlp architecture for vision. *Advances in Neural Information Processing Systems*, 34:24261–24272, 2021. 12

[51] Du Tran, Heng Wang, Lorenzo Torresani, and Matt Feiszli. Video classification with channel-separated convolutional networks. In *ICCV*, pages 5552–5561, 2019. 5

[52] Du Tran, Heng Wang, Lorenzo Torresani, Jamie Ray, Yann LeCun, and Manohar Paluri. A closer look at spatiotemporal convolutions for action recognition. In *CVPR*, pages 6450–6459, 2018. 4, 6

[53] Aaron Van den Oord, Yazhe Li, and Oriol Vinyals. Representation learning with contrastive predictive coding. *arXiv e-prints*, pages arXiv–1807, 2018. 3, 4

[54] Ashish Vaswani, Noam Shazeer, Niki Parmar, Jakob Uszkoreit, Llion Jones, Aidan N Gomez, Łukasz Kaiser, and Illia Polosukhin. Attention is all you need. In *NeurIPS*, pages 5998–6008, 2017. 4

[55] Limin Wang, Wei Li, Wen Li, and Luc Van Gool. Appearance-and-relation networks for video classification. In *CVPR*, 2018. 6

[56] Limin Wang, Zhan Tong, Bin Ji, and Gangshan Wu. Tdn: Temporal difference networks for efficient action recognition. In *CVPR*, pages 1895–1904, 2021. 6, 7

[57] Mengmeng Wang, Jiazheng Xing, and Yong Liu. Actionclip: A new paradigm for video action recognition. *arXiv preprint arXiv:2109.08472*, 2021. 2, 4, 5, 7, 8

[58] Xiaolong Wang, Ross Girshick, Abhinav Gupta, and Kaiming He. Non-local neural networks. In *CVPR*, pages 7794–7803, 2018. 5

[59] Xiaohan Wang, Linchao Zhu, and Yi Yang. T2vlad: global-local sequence alignment for text-video retrieval. In *CVPR*, pages 5079–5088, 2021. 4

[60] Wenhao Wu, Dongliang He, Tianwei Lin, Fu Li, Chuang Gan, and Errui Ding. Mvfnet: Multi-view fusion network for efficient video recognition. In *AAAI*, volume 35, pages 2943–2951, 2021. 5, 6, 7

[61] Wenhao Wu, Dongliang He, Xiao Tan, Shifeng Chen, and Shilei Wen. Multi-agent reinforcement learning based frame sampling for effective untrimmed video recognition. In *ICCV*, pages 6222–6231, 2019. 5

[62] Wenhao Wu, Yuxiang Zhao, Yanwu Xu, Xiao Tan, Dongliang He, Zhikang Zou, Jin Ye, Yingying Li, Mingde Yao, Zichao Dong, et al. Dsanet: Dynamic segment aggregation network for video-level representation learning. *ACM MM*, pages 1903–1911, 2021. 5

[63] Boyang Xia, Zhihao Wang, Wenhao Wu, Haoran Wang, and Jungong Han. Temporal saliency query network for efficient video recognition. *ECCV*, pages 741–759, 2022. 5

[64] Boyang Xia, Wenhao Wu, Haoran Wang, Rui Su, Dongliang He, Haosen Yang, Xiaoran Fan, and Wanli Ouyang. Nsnet: Non-saliency suppression sampler for efficient video recognition. *ECCV*, pages 705–723, 2022. 5

[65] Saining Xie, Chen Sun, Jonathan Huang, Zhuowen Tu, and Kevin Murphy. Rethinking spatiotemporal feature learning: Speed-accuracy trade-offs in video classification. In *ECCV*, pages 305–321, 2018. 4, 6

[66] Shen Yan, Xuehan Xiong, Anurag Arnab, Zhichao Lu, Mi Zhang, Chen Sun, and Cordelia Schmid. Multiview transformers for video recognition. In *CVPR*, pages 3333–3343, 2022. 5

[67] Jianwei Yang, Chunyuan Li, Pengchuan Zhang, Bin Xiao, Ce Liu, Lu Yuan, and Jianfeng Gao. Unified contrastive learning in image-text-label space. In *CVPR*, pages 19163–19173, 2022. 4

[68] Jiahui Yu, Zirui Wang, Vijay Vasudevan, Legg Yeung, Mojtaba Seyedhosseini, and Yonghui Wu. Coca: Contrastive captioners are image-text foundation models. *arXiv preprint arXiv:2205.01917*, 2022. 4

[69] Lu Yuan, Dongdong Chen, Yi-Ling Chen, Noel Codella, Xiyang Dai, Jianfeng Gao, Houdong Hu, Xuedong Huang, Boxin Li, Chunyuan Li, et al. Florence: A new foundation model for computer vision. *arXiv preprint arXiv:2111.11432*, 2021. 4, 5

[70] Xiaohua Zhai, Alexander Kolesnikov, Neil Houlsby, and Lucas Beyer. Scaling vision transformers. In *arXiv preprint arXiv:2106.04560*, 2021. 5

[71] Bowen Zhang, Jiahui Yu, Christopher Fifty, Wei Han, Andrew M Dai, Ruoming Pang, and Fei Sha. Co-training transformer with videos and images improves action recognition. *arXiv preprint arXiv:2112.07175*, 2021. 5

[72] Shuai Zhao, Linchao Zhu, Xiaohan Wang, and Yi Yang. Centerclip: Token clustering for efficient text-video retrieval. *SIRIR*, 2022. 4

[73] Kaiyang Zhou, Jingkang Yang, Chen Change Loy, and Ziwei Liu. Learning to prompt for vision-language models. *arXiv preprint arXiv:2109.01134*, 2021. 13

## Appendix

In this appendix, §A contains *results* of our method for image recognition. §B contains further *results* for video recognition: the training details (§B.1), more ablations (§B.2), and more visualizations of different classifier (§B.3). §C contains additional *details* for: the statistics of video datasets (§C.1), visual encoder architectures (§C.2), Batch Gather (§C.3), LDA (§C.4) and data overlaps (§C.5).

### A. Experiments: Image Recognition

We also evaluate our approach to the image recognition task. Here we conduct experiments on ImageNet [9] which contains 1000 categories and 1.2 million images. Note that our goal here is to observe how well our method works, not to pursue a higher top-1 accuracy. Instead of a large epoch (*i.e.*, 300 epochs), complex augmentation (*i.e.*, Gaussian Blur, Solarization, MixUp, *etc*) and various optimization tricks, we train models on ImageNet with only **10 epochs** and the most basic augmentation (*i.e.*, Random Crop).

**Few-shot image recognition.** Here we also use the challenging  $K$ -shot  $C$ -way setting on ImageNet. Specifically, the models are trained using  $K$  images (shots) from the training set for each image category and then measure performance on the corresponding standard 1000-class testing set. As shown in Table A.1, the results reveal that our method has strong transferability under data-poor conditions, whereas the standard unimodality paradigm is ineffective in comparison to ours.

K-shot	0	1	3	5	All
Vision-Only	0	51.6	63.8	66.3	79.7
Ours	66.7	71.5	73.1	74.6	82.3

Table A.1. Few-shot image recognition on ImageNet. “Zero-shot” and “All-shot” denote the lower and upper bounds of the task respectively. Top-1 accuracy is reported here.

**Efficient training.** For readers’ reference, we provide the performance of our approach with different visual backbones on ImageNet in Tabel A.2. Notably, using 8 GPUs, we can train the ViT-L/14 only takes 6 hours to achieve 86.7%. Here, we show the results of ViT-L model trained with our method for 10 epochs compared with other methods [18, 50] trained with 300 epochs as follows. We can see that our approach can significantly speed up convergence.

### B. Additional Results on Video Recognition

#### B.1. Training details

**General video recognition:** In Table A.3, we present our training details for general video recognition. We share the

Backbone	Top-1	Epoch	A100-days
DeiT ViT-L	84.9	300	-
MLP-Mixer ViT-L	85.3	300	-
Ours ViT-L	86.7	10	2.0
Ours ViT-L (336↑)	87.5	10	5.7

Table A.2. Comparisons on image recognition. Our models are trained with 10 epochs.

same recipe on all the video datasets, *i.e.*, Kinetics-400, ActivityNet, HMDB-51, UCF-101.

**Few-shot video recognition:** We repeat the samples to keep the same iterations with the above general counterpart. For example, we train the model on Kinetics-400 with  $\sim$ 900 iterations per epoch for general setting, we repeat the sample to maintain the same  $\sim$ 900 iterations per epoch for few-shot setting. In this way, we only the few-shot models with 2 epochs on Kinetics-400, and 10 epochs on other video datasets, *i.e.*, ActivityNet, HMDB-51, UCF-101. Other settings are same with the Table A.3.

**Zero-shot video recognition:** We use the Kinetics-400 pre-trained models to directly perform cross-dataset zero-shot video recognition **without any additional training** on other datasets *i.e.*, ActivityNet, HMDB-51, UCF-101 and Kinetics-600.

Setting	Value
<i>Training Hyperparameter</i>	
Batch size	256
Vocabulary size	49408
Training epochs	30
Optimizer	AdamW
Learning rate (base, minimal)	(5e-5, 5e-6), cosine
Weight decay	0.2
Linear warm-up epochs	5
Adam $\beta_1, \beta_2$	0.9, 0.98
<i>Augmentation</i>	
Resize	RandomSizedCrop
Crop size	224 (Default)
Random Flip	0.5
Random Gray scale	0.2
RandAugment	$N = 2, M = 9$

Table A.3. Default training details for video recognition

#### B.2. More ablations on Kinetics-400.

**Comparison with vision-only framework.** As shown in Figure A.3, our method surpasses *Vision-Only* baselines across multiple label fractions on Kinetics-400, especially when only 10% labeled data is available for training, demonstrating that the advantage of our method is more

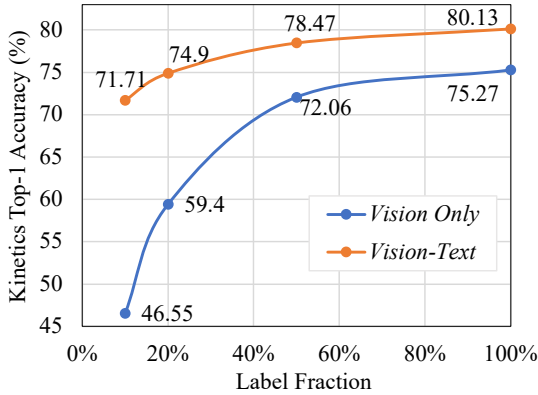


Figure A.3. Vision-Text *vs.* Vision-only framework under different label fractions on Kinetics-400.

profound when the labeled data is limited. Also, when training with full data, our *Vision-Text* method leads to an additional 5% improvement with the same training recipe. Figure A.4 further demonstrates our paradigm significantly improves convergence speed.

**Text input forms.** We study several text input forms in Table A.4, including class names, single hard template, multiple hard templates, and learnable templates. More details are as follows:

*Class name.* To build textual embeddings, we utilize the category names of the dataset as the text input, *e.g.*, “*eating hotdog*”, “*driving car*”, *etc.* We can see that only using the label text can yield good results.

*Single hard template.* We employ the hand-crafted template “*a video of a person {class name}*.” to form a sentence as input. This only slightly increases performance over the baseline of using the label text.

*Multiple hard templates.* CLIP<sup>4</sup> provides 28 templates for Kinetics, one of which is the above single template. We use these multiple templates as the text augmentation during training. At each iteration, we choose one template at random as text input. Then we perform the evaluation using the single template as input. Performance decreases by 0.64% on Kinetics-400. This may be because various prompt templates may introduce extra noise for the training.

*Learnable templates.* We adopt the automated prompt CoOp [73] to describe a prompt’s context using a set of learnable vectors. Specifically, the prompt given to the text encoder is designed with the following form,

$$t = [\mathbf{V}]_1 [\mathbf{V}]_2 \dots [\mathbf{V}]_M [\text{class name}], \quad (7)$$

where each  $[\mathbf{V}]_m$  ( $m \in \{1, \dots, M\}$ ) is a vector of the same size as word embeddings, and  $M$  is the number of context tokens. We set the  $M$  to 4. The results suggest that different templates have little impact on our model.

<sup>4</sup><https://github.com/openai/CLIP/blob/main/data/prompts.md>

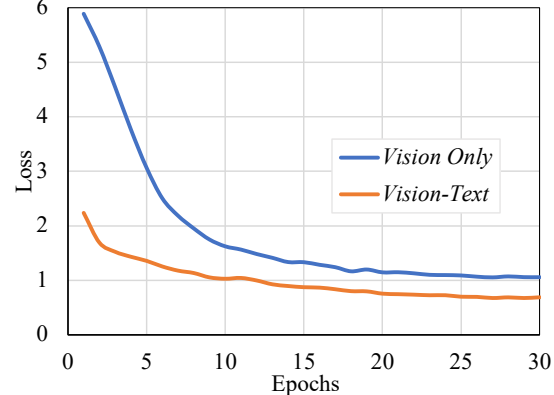


Figure A.4. The training loss of Vision-Text and Vision-only framework on Kinetics-400.

Text input form	Top-1
class name	81.4
“a video of a person” + class name	<b>81.5</b>
multiple fixed templates + class name	80.9
learnable template + class name	81.2

Table A.4. Study on various text input forms.

### B.3. More visualizations of different classifiers

Here we provide more visualizations of different classifiers in Figure A.5.

## C. Additional Details

### C.1. Statistics of video datasets

**Kinetics-400** [26] is a large-scale video dataset, which consists of 240k training videos and 20k validation videos in 400 different human action categories. Each video in the dataset is a 10-second clip of action moment annotated from raw YouTube video.

**Kinetics-600** [5] is an extension of Kinetics-400. Kinetics-600 consists of around 480k videos from 600 action categories. The 480K videos are divided into 390k, 30k, 60k for training, validation and test sets, respectively. In this paper, we use its test set for zero-shot evaluation.

**UCF-101** [48] contains 13k videos spanning over 101 human actions.

**HMDB-51** [29] contains approximately 7k videos belonging to 51 action class categories.

**ActivityNet-v1.3** [4] is a large-scale untrimmed video benchmark, contains 19,994 untrimmed videos of 5 to 10 minutes from 200 activity categories.

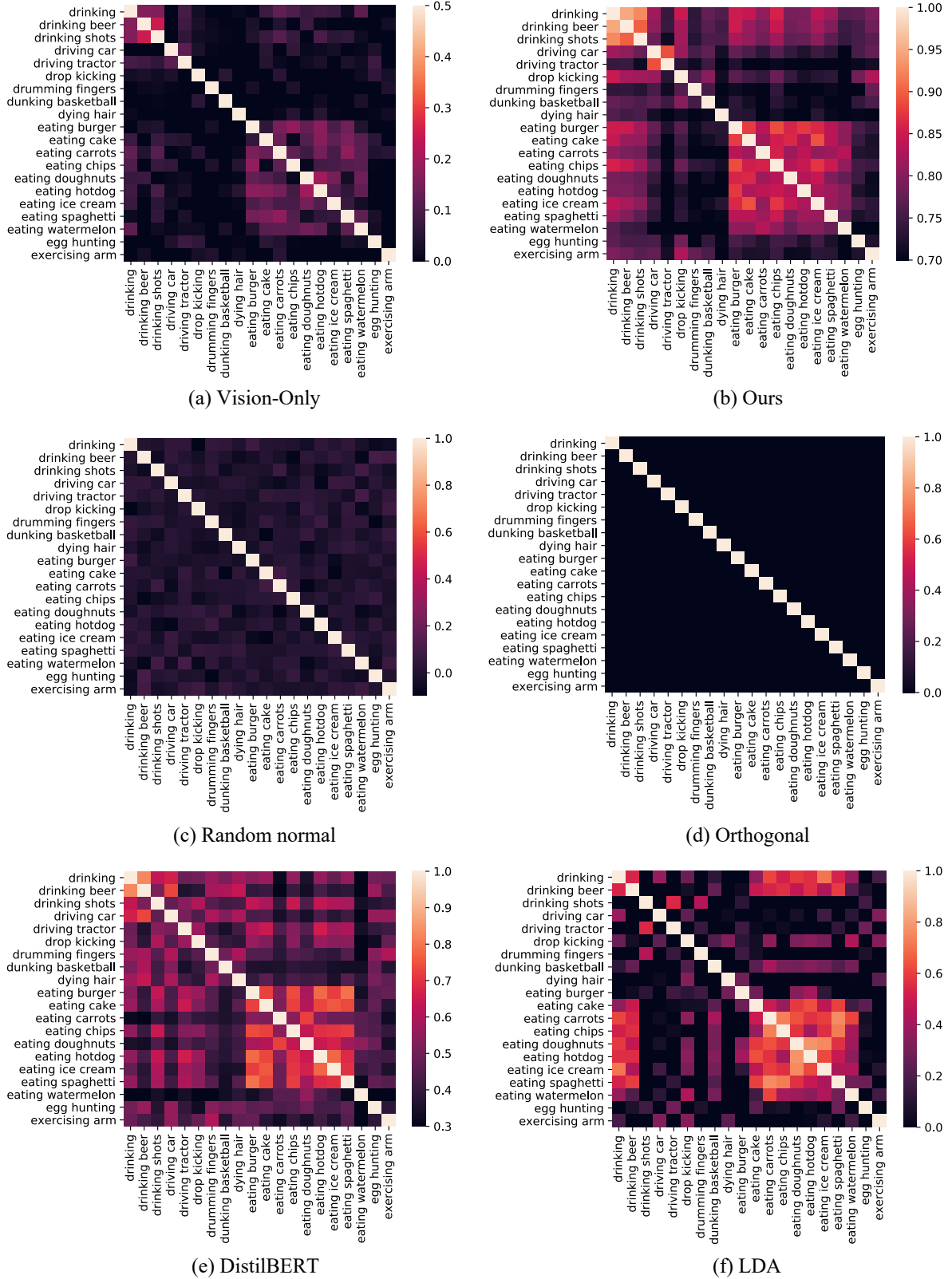


Figure A.5. Inter-class correlation maps of “embeddings of class labels” for 20 categories on Kinetics-400. The color thresholds are adjusted for better understandability. Please zoom in for best view.

Model	Embedding	Input	ResNet		Text Transformer		
	dimension	resolution	blocks	width	layers	width	heads
RN50	1024	224	(3, 4, 6, 3)	2048	12	512	8

Table A.5. CLIP-ResNet hyperparameters

Model	Embedding	Input	Vision Transformer			Text Transformer		
	dimension	resolution	layers	width	heads	layers	width	heads
ViT-B/32	512	224	12	768	12	12	512	8
ViT-B/16	512	224	12	768	12	12	512	8
ViT-L/14	768	224	24	1024	16	12	768	12
ViT-L/14-336px	768	336	24	1024	16	12	768	12

Table A.6. CLIP-ViT hyperparameters

## C.2. Visual encoder architectures

We provide the full architecture details of the visual encoder and textual encoders in this paper. Table A.5 shows the CLIP-ResNet architectures. Table A.6 shows the CLIP-ViT architectures.

## C.3. Batch Gather for Distributed InfoNCE

Instead of Data-Parallel Training (DP), which is single-process, multi-thread, and only works on a single machine, Distributed Data-Parallel Training (DDP) is a widely adopted single-program multiple-data training paradigm for single- and multi-machine training. Due to GIL contention across threads, per-iteration replicated model, and additional overhead introduced by scattering inputs and gathering outputs, DP is usually slower than DDP even on a single machine. Hence, we develop the Distributed InfoNCE based on DDP for large batch size and fast training. The core of the Distributed InfoNCE implementation is batch gathering. Say there are  $M$  GPUs and each GPU gets  $N$  input pairs, we need to calculate the  $NM \times NM$  similarity matrix across the GPUs for InfoNCE loss. Without batch gathering, each GPU only computes a local  $N \times N$  matrix, *s.t.*  $N \ll NM$ , Then the cosine similarity and the InfoNCE loss would be calculated only for the pairs within a single GPU and later their gradients would be averaged and synced. That's obviously not what we want.

The batch gathering for Distributed InfoNCE is presented as follows. When calculating the similarity matrix (and thus the logit scores across text inputs for each image/video), a GPU only needs to hold  $M$  vision features, and perform matrix product with  $NM$  text features, yielding an  $M \times NM$  matrix. This computation is distributed (*i.e.*, sharded) across  $N$  GPUs, and we have calculated  $NM \times NM$  similarities across the GPUs in total. The loss we employ is symmetric and the same happens *w.r.t.* text inputs. As shown in Algorithm 1, we also give an example pseudocode

to help you understand the statement.

## C.4. LDA classifier

Here we provide the details of LDA classifier. We directly use the official CLIP-pretrained visual encoder to extract video embeddings, and the visual encoder is not finetuned on Kinetics-400. Then we perform LDA on the pre-extracted video embeddings of the training set in Kinetics-400 to initialize  $W$  and freeze it for finetuning the visual encoder on the Kinetics-400 dataset.

LDA is commonly used for feature classification or feature dimensionality reduction. However, in this work, we only use LDA for feature classification (in order to get “discriminant coefficients” as the classifier) instead of feature dimensionality reduction. For better understanding, we show the code in Algorithm 2 which generates the LDA coefficient and there is no dimension reduction.

## C.5. Discussion on data overlaps

In this paper, we mainly focus on the video recognition task with the Kinetics dataset. As shown in Fig.17 of CLIP official paper, CLIP has done the data overlap analysis on the Kinetics-700 dataset. They observe that there are less than 1% overlaps and many overlaps on Kinetics-700 are in fact all black transition frames. Then they conduct the experiment on overlapping data. The results show that the Kinetics-700 has no performance improvement, and even has an apparent 20% accuracy drop on the overlapping data. Therefore, the use of data in this paper is reasonable.

---

**Algorithm 1** Numpy-like Pseudocode that illustrates the role of Batch Gather in Distributed InfoNCE.

---

```
1  # text_encoder: encoder network for text input
2  # vision_encoder: encoder network for vision input, e.g., images or videos.
3  # V: minibatch of vision inputs
4  # T: minibatch of text inputs
5  # N: the local batch size of each GPU, e.g., 16
6  # M: the number of GPUs, e.g., 8
7  # N * M: the global batch size for multi-gpu training, e.g., 128
8
9  # extract feature representations of each modality
10 local_vision_features = vision_encoder(V) # shape: [N, embed_dim]
11 local_text_features = text_encoder(T) # shape: [N, embed_dim]
12
13 # normalization
14 local_vision_features = 12_normalize(local_vision_features, axis=1)
15 local_text_features = 12_normalize(local_text_features, axis=1)
16
17 # batch_gather is a function gathering and concatenating the tensors across GPUs.
18 all_vision_features = batch_gather(local_vision_features) # shape: [N * M, embed_dim]
19 all_text_features = batch_gather(local_text_features) # shape: [N * M, embed_dim]
20
21 # scaled pairwise cosine similarities
22 # shape = [N, N * M]
23 logits_vision = logit_scale * local_vision_features @ all_text_features.t()
24 # shape = [N, N * M]
25 logits_text = logit_scale * local_text_features @ all_vision_features.t()
26
27 # The logits are then used as inputs for N*M-way (e.g., 128-way) classification,
28 # resulting in a loss value corresponding to N inputs in each GPU.
29 # Then Distributed Data Parallel mechanism takes care of averaging these across GPUs,
30 # which becomes equivalent to calculating the loss over NMxNM (e.g., 128x128) similarities.
31
```

---

---

**Algorithm 2** The code generates the LDA coefficient for Kinetics-400 dataset.

---

```
1  import numpy as np
2  from sklearn.discriminant_analysis import LinearDiscriminantAnalysis as LDA
3  input = np.load('feats_labels_400class.npz') # pre-extracted visual features
4  feats = input['feats'] # size: [24000, 512]
5  labels = input['labels'] # size: [24000,]
6  lda = LDA()
7  lda.fit(feats, labels)
8  classifier = lda.coef_ # size: [400, 512]
9
```

---